



HAL
open science

Experimental and modeling study of burning velocities for alkyl aromatic components relevant to diesel fuels

Marco Mehl, Olivier Herbinet, Patricia Dirrenberger, Roda Bounaceur, Pierre-Alexandre Glaude, Frédérique Battin-Leclerc, William J. Pitz

► To cite this version:

Marco Mehl, Olivier Herbinet, Patricia Dirrenberger, Roda Bounaceur, Pierre-Alexandre Glaude, et al. Experimental and modeling study of burning velocities for alkyl aromatic components relevant to diesel fuels. Proceedings of the Combustion Institute, 2015, 35, pp.341 - 348. 10.1016/j.proci.2014.06.064 . hal-01099836

HAL Id: hal-01099836

<https://hal.science/hal-01099836v1>

Submitted on 5 Jan 2015

HAL is a multi-disciplinary open access archive for the deposit and dissemination of scientific research documents, whether they are published or not. The documents may come from teaching and research institutions in France or abroad, or from public or private research centers.

L'archive ouverte pluridisciplinaire **HAL**, est destinée au dépôt et à la diffusion de documents scientifiques de niveau recherche, publiés ou non, émanant des établissements d'enseignement et de recherche français ou étrangers, des laboratoires publics ou privés.

Experimental and modeling study of burning velocities for alkyl aromatic components relevant to diesel fuels

Marco Mehl¹, Olivier Herbinet², Patricia Dirrenberger², Roda Bounaceur², Pierre-Alexandre Glaude², Frédérique Battin-Leclerc², William J. Pitz¹

¹Lawrence Livermore National Laboratory, Livermore, CA 94551, USA

²Laboratoire Réactions et Génie des Procédés, UMR 7274 CNRS, Université de Lorraine, 54001 Nancy, France

Abstract

Aromatic species represent a significant fraction (about one third by weight) of both diesel and gasoline fuels. Much of the aromatics in diesel and gasoline are alkyl-benzene species. Although toluene, the lightest of the alkyl-benzenes, has been the subject of extensive literature investigations, very little experimental data are available for heavier alkyl-benzenes (9–20 carbon atoms) relevant to diesel fuel.

In this work, the burning velocity of ethyl-, n-propyl- and n-butyl-benzenes were measured in a premixed flat-flame burner using the heat flux method. The burning velocities were measured as a function of the equivalence ratio at atmospheric pressure and for two unburned gas temperatures (358 and 398 K). These new experiments are compared with burning velocities for toluene previously measured by the authors. The comparisons showed that ethyl-benzene has the highest flame speed, followed by n-propyl- and n-butyl-benzenes which have similar burning velocities. Toluene has the lowest flame speed. Excellent agreement was observed between the new measurements and simulations using a mechanism for alkyl-benzenes recently published by Lawrence Livermore National Laboratory (LLNL) and National University of Ireland.

Based on the strong correlation between experiments and calculations, different aspects contributing to the burning speed of the fuels (thermal effects, kinetics, ...) were analyzed using the model. A sensitivity analysis was used to determine the reaction rate constants that are most important in determining the flame speed. Reaction path analysis and species profiles in the flame were used to identify the key reaction paths that lead to increase or decrease in the burning velocities. Contrary to what is generally observed for alkanes whose flame speed is controlled by small radical fragments, the flame speed of aromatics is influenced by fuel specific intermediates such as phenyl, benzyl, or even heavier species. The new experimental data and modeling insight generated by this work will support the development of models for heavier alkyl-aromatics of great relevance to diesel fuel.

Keywords: Kinetic modeling; Toluene; Ethyl-benzene; Propyl-benzene; Butyl-benzene

Corresponding author: Marco Mehl, 7000 East Ave L-288, Livermore, CA 94550, USA. Fax: +1 925 423 5808. E-mail: mehl6@llnl.gov.

1. Introduction

Diesel fuels are complex blends of hundreds of species which include a broad range of hydrocarbons derived from distillation of crude oil and oxygenated molecules used as additives [1,2]. The main classes of molecules found in petroleum-based diesel fuels are *n*- and *iso*-paraffins, naphthenes and aromatic compounds with carbon atom numbers ranging from 10 to 22 (with an average around 14-15) [1]. Each of the three molecular classes comprises about one-third by weight of diesel fuels depending on the origin and treatments of crude oil.

The aromatic fraction of diesel fuels usually consists of single ringed species with one or several side alkyl chains although alkylated double ringed compounds can be found in significant concentrations [2,3]. The study presented in this paper focuses on burning velocities of species representative of the aromatic class of molecules found in diesel fuels: alkyl-benzenes.

Within this class of compounds, *n*-propyl-benzene and *n*-butyl-benzene have received significant attention due to their consideration as surrogate aviation fuel components, as demonstrated by the many experimental and modeling studies [4-9]. Although the boiling point of C₉-C₁₀ aromatics falls in the low end of the boiling range of diesel fuels, the chemistry of these components is considered to be archetypical for their class, as indicated by Pitz and Mueller [2] and other studies [10-12].

Laminar burning velocities are important parameters in many areas of combustion science such as the design of burners or engines and for the prediction of explosions. There are limited experimental data in the literature about laminar flame velocities of alkyl-benzenes with more than 8 carbon atoms. Hui et al. studied the oxidation of *n*-propyl-benzene using a twin-flame counterflow setup [4]. Laminar flame velocities of fuel-air mixtures were carried out at atmospheric pressure, at two temperatures (400 and 470 K) and at equivalence ratios ranging from 0.7 to 1.4. The same paper reports the laminar flame velocities of toluene and 1,2,4- and 1,3,5-trimethyl-benzenes at the same conditions for comparison purpose. Ji et al. also measured laminar flame velocities of *n*-propyl-benzene-air mixtures using the counterflow flame configuration [5]. Experiments were performed at atmospheric pressure, at 353 K and over the equivalence ratio 0.7–1.5. They also measured laminar flame velocities of benzene, toluene, the three xylene isomers, and 1,2,4- and 1,3,5-trimethyl-benzenes under the same conditions. These studies revealed that *n*-propyl-benzene laminar flame velocities are lower than that of benzene but faster than that of toluene, xylenes and trimethyl-benzenes. The extensive kinetic analysis presented in Hui and Ji works [4,5] concluded that the flame chemistry of this class of compounds is influenced by the first intermediates formed along the oxidation process of the fuel and, in particular, the formation of resonantly-stabilized benzyl radicals.

In order to supplement the existing set of fundamental data and complement Ji et al. and Hui et al. works [4,5], the burning velocities of increasingly heavy alkyl-benzenes were measured in a premixed flat-flame burner across a wide range of equivalence ratios and temperatures (358–398 K) at atmospheric pressure using the heat flux method. The experimental results were finally analyzed using a recently published detailed kinetic mechanism. This two-fold approach allows to highlight critical aspects dictated by the kinetics of the fuels and to extrapolate information useful to compile detailed mechanisms for this class of compounds.

2. The Experimental apparatus

Measurements of laminar flame velocity were performed using the heat flux method [13] using a flat-flame adiabatic burner which was built following the design proposed by de Goey and coworkers [14-17]. It was recently used to measure laminar flame velocities for components of natural gas [18] and the laminar burning velocity of gasoline fuels with addition of ethanol [19]. The flat flame adiabatic burner used in this study consists of a burner head mounted on a plenum chamber. The burner head

is a thin perforated plate made of brass of 30 mm diameter which is used to stabilize the flame. Each small hole of the plate has a 0.5 mm diameter and the pitch between the holes is 0.7 mm. Eight type K thermocouples of 0.5 mm diameter are soldered into the plate surface and are positioned at different distances and angles from the center to the periphery of the burner. The plenum chamber is surrounded by a heating jacket that enables the control of the temperature of the fresh gases (from ambient up to 398 K). The edge of the burner plate is heated at a higher temperature than the one of the fresh gases (about 50 K higher) to keep the temperature of the burner plate constant and to heat up the mixture when it flows through the plate at a higher temperature than the unburned gas mixture. Thus, the heat gain of the unburned gas mixture can compensate for the heat loss necessary for stabilizing the flame. Thermocouple temperature measurements are used to assess the amount of the heat loss or gain. Two thermostatic oil baths provide the heat transfer fluid to the heating and cooling jackets of the burner.

If the gas velocity is lower than the adiabatic flame burning velocity, the sum of the heat loss and heat gain is larger than zero. Then, the center of the burner plate is hotter than the periphery, and the flame is stabilized under subadiabatic conditions. On the other hand, if the unburned gas velocity is larger than the adiabatic burning velocity, the center of the burner plate is cooler than the periphery and the flame is stabilized under superadiabatic conditions. Thus, when the burner head temperature profile is flat, it means that no heat is lost or gained by the flame so that the flame becomes adiabatic. By changing the flow rate of the gas mixture, it is also possible to find an appropriate value of the gas velocity to cancel out the net heat flux so that the radial temperature distribution in the burner plate is uniform and equal to the temperature of the heating jacket. The flow rate at which the net heat flux is zero corresponds to the adiabatic flame burning velocity.

Gas flow rates were controlled using Bronkhorst High-Tech Mass Flow Controllers. Oxygen and nitrogen were delivered by Messer. The purity of these two gases was 99.995%. For liquid fuels, flow rates were measured using a Bronkhorst mini-CORI-FLOW Mass Flow Controller coupled to an evaporator. Good agreement for measured laminar burning velocities of liquid fuels (*n*-heptane, *iso*-octane and toluene) [19] with most of the experimental data from the literature demonstrated the reliability of the evaporator for liquid fuels.

Ethyl-benzene ($\geq 99\%$) and *n*-propyl-benzene ($\geq 98\%$) were provided by Sigma–Aldrich. *n*-Butyl-benzene ($\geq 99\%$) was provided by ACROS. As the adiabatic laminar burning velocity is found when the net heat loss is zero, the uncertainties are only dependent on a few factors. The uncertainty in the laminar burning velocity can be attributed to the error in the mass flow measurements (around 0.5% for each MFC) which can lead to a global uncertainty of 1.5% in the laminar flame velocity, the error in the reading of the temperature with thermocouples which could lead to an uncertainty of around 0.2 cm/s in the laminar flame velocity, and to errors due directly to flame distortions, such as edge effects for example (around 0.2 cm/s). Concerning the determination of equivalence ratios, note that the main uncertainty is due to the error in the mass flow measurements which leads to an error of about 1%. Finally, there are some qualitative errors which are difficult to evaluate such as the possible uncertainties in the fresh gas temperature if the gaseous mixture does not spend enough time in the plenum chamber to uniformly reach the studied temperature (358 or 398 K). Possible errors related in the fuel purity are minute since high purity gases are used.

3. Experimental and modeling results

The apparatus here described was used to measure laminar flame velocities of various aromatic compounds (at ambient condition) relevant to gasoline and diesel fuels. Experiments were performed at atmospheric pressure, at different fresh gas temperatures in the range 298–398 K, and using synthetic air (79% (vol) nitrogen and 21% (vol) oxygen). Data obtained in this study were systematically compared with data from the literature when available.

Laminar flame velocities have been measured for three alkyl-benzenes: ethyl-, *n*-propyl- and *n*-butyl-benzenes. The range of conditions at which measurements were possible (temperature, equivalence ratio) was narrowed due to the low vapor pressure of these types of hydrocarbons. As an example, laminar flame velocities of ethyl-benzene and heavier species could not be acquired at 298 K. Figures 1 to 3 display the laminar flame velocities obtained in this study for the three alkyl-benzenes: ethyl-benzene, *n*-propyl-benzene and *n*-butyl-benzene.

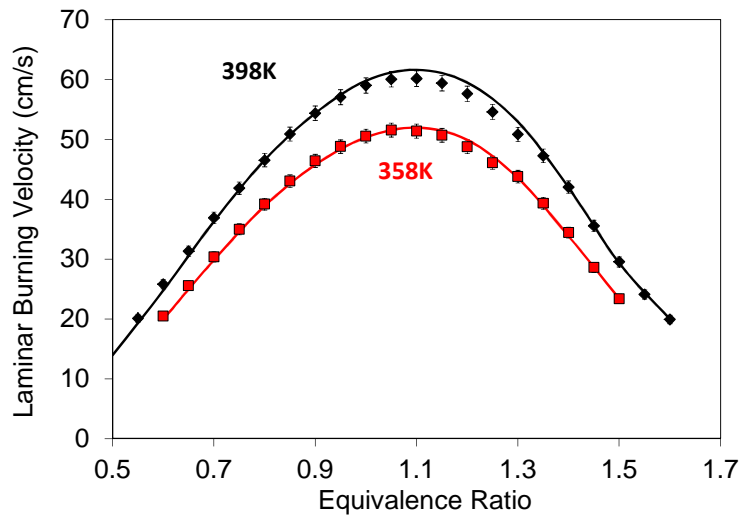


Figure 1: Laminar flame velocities as a function of equivalence ratio for ethyl-benzene/air mixtures at two fresh gas temperatures (358–398 K) at atmospheric pressure. Symbols are experimental data and lines simulations.

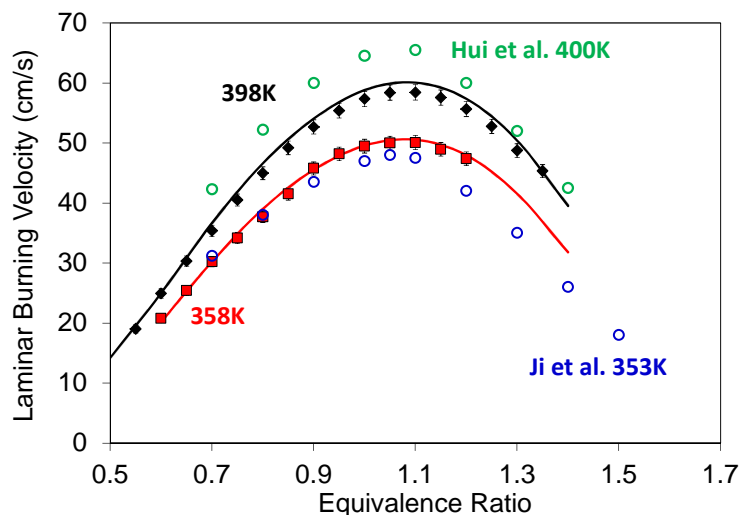


Figure 2: Laminar flame velocities as a function of equivalence ratio for *n*-propyl-benzene at two fresh gas temperatures (358 and 398 K). Symbols are experimental data and lines simulations performed using the LLNL model. Empty symbols refer to experimental data from Hui et al. [4] and Ji et al. [5].

The *n*-propyl-benzene data have been compared with data from Ji et al. at 353 K [5] and Hui et al. at 400 K [4] in the counter flow configuration. Good agreement is observed with data from Ji et al. [5] for equivalence ratios below 0.8. Above 0.8, laminar flame velocities from Ji et al. are slower than our data with discrepancies in the order of 10% at 1.2, the richest conditions at which we were able to collect reliable data. Data published by Hui et al. at 400 K strongly disagree with our data obtained at 398 K: their laminar flame velocities are faster, especially at equivalence ratios lower than 1.2. The observed

discrepancies between the different sets of data suggest that further experimental studies are needed to confirm the values of laminar flame velocities for *n*-propyl-benzene. It should be noted, however, that the method used in the present study does not require any extrapolation as measurements are carried out from an un-stretched flame whereas counter-flow measurements are sensitive to differences in the approaches of how the data is extrapolated to an un-stretched flame. No literature data were available for ethyl-benzene and *n*-butyl-benzene.

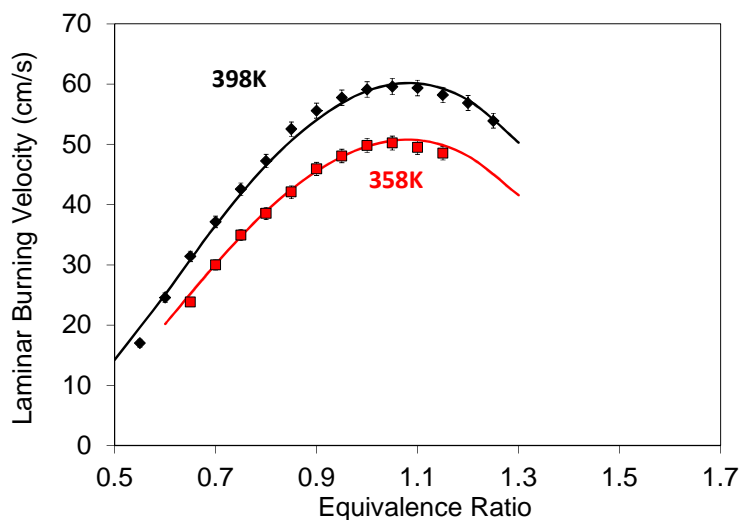


Figure 3: Laminar flame velocities as a function of equivalence ratio for *n*-butyl-benzene at two fresh gas temperatures (358 and 398 K). Symbols are experimental data and lines simulations LLNL model.

Figures 1 to 3 also compare the experimental data of the three *n*-alkyl-benzenes with numerical results computed using the recently published detailed kinetic developed at Lawrence Livermore National Laboratory (LLNL) for this class of compounds [20-23]. The model is based on the toluene mechanism from Metcalfe et al. [24], which is the result of an extensive literature review incorporating reaction pathways and rates from seminal works from many institutions (Princeton, KIT, UIC, Argonne, NIST, NJIT, CNRS, ...). The mechanism here adopted has the important advantage, over other literature mechanisms, of including all the fuel molecules included in this study: this feature allows comparison of the fuel kinetics based on the same base chemistry for small radicals. Moreover, the kinetic mechanism for ethyl, *n*-propyl and *n*-butyl-benzenes was developed following a hierarchical approach adopting similar reaction rate rules for all fuels, ensuring that the relative reactivity is predicted through a systematic approach which is less sensitive to choices of the rate constants. The alkyl-benzene mechanism was previously validated by comparing computed results to experimental ignition delay times from shock tubes and rapid compression machines over a wide range of conditions [20-23]. Speciation measurement from flow reactors and stirred reactors were also used to validate the mechanism. Good agreement was obtained for these previous comparisons.

Transport properties for the toluene submechanism are from Metcalfe et al. [24] while the ones for newly introduced species have been calculated from the critical parameter of the corresponding species or of species with similar structural features. Further details are available in the attached transport file.

The flame calculations were performed in Chemkin Pro[®] using a typical grid-size of about 250 points. Grid convergence was tested by doubling the number of grid point without noticing significant changes in the solution (<0.8%). Results from the chemical kinetic model showed excellent quantitative agreement (± 1.5 cm/s) with the new experimental data presented in this paper for all the considered fuels. For previous published data on toluene, the model slightly overpredicts the measured flame speeds (>1.5 cm/s) for equivalence ratios between 1.1 and 1.3.

In order to systematically analyze the experimental and numerical results, the burning velocities of the different fuels were compared at similar conditions. Figure 4 displays the comparison of experimentally-measured and calculated laminar-flame velocities of alkyl-benzenes from toluene up to *n*-butyl-benzene at 358 K. Toluene data used in this comparison are from a previous study [19].

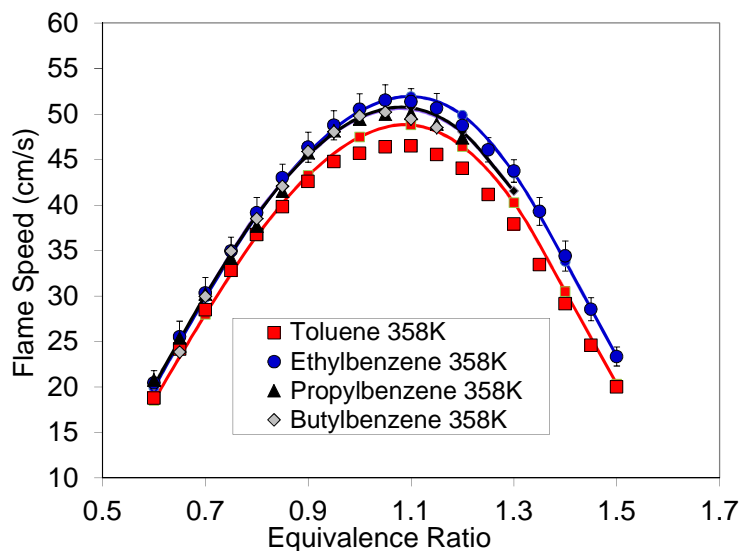


Figure 4: Comparison of laminar flame velocities (symbols: experiments, lines: calculations) as a function of equivalence ratio for alkyl-benzenes from toluene up to *n*-butyl-benzene at 358 K. Toluene data are from a previous study [12]. The lines for propyl-benzene and butyl-benzene overlap.

It can be seen that at lean conditions the laminar burning velocities of ethyl-, *n*-propyl- and *n*-butyl-benzenes are similar and that laminar flame velocities of toluene are slower than the ones of the three other fuels. At equivalence ratios larger than 0.9, ethyl-benzene appears to be the fuel having the fastest flame speed while *n*-propyl-benzene and *n*-butyl-benzene profiles look nearly identical (note how they overlap in Figure 4) laying between the curves of the two lighter fuels.

4. Kinetic analysis

Based on the consistency between experimental measurements and numerical results the LLNL kinetic model was used to investigate the trends in the flame speed rates highlighted by the experiment: ethyl-benzene shows the highest flame speed, followed by *n*-propyl- and *n*-butyl-benzenes which have similar burning velocities, followed by toluene, which has the lowest flame speed (Figure 4).

Burning velocities of hydrocarbons are largely controlled by the thermodynamic properties of the fuel and by small radical chemistry (a reliable C_0 - C_1 mechanism is mandatory to correctly reproduce the flame front chemistry relevant to the flame propagation). The differences observed in this set of experiments however are not easily explained only on the base of C_0 - C_1 chemistry but appears to be fuel specific. One peculiar aspect of aromatic species is the potential to form stable radicals as already pointed out by Ji et al. [5]. In the course of this study, we will analyze how the rate of formation and the character of these slow reacting species play an important role in determining the observed trend.

The first aspect considered in this study is the flame temperature of the fuels: higher adiabatic flame temperatures are typically associated with faster burning rates. The calculated flame temperatures for these fuels are represented in Figure 5, panel b, solid bars for $\Phi = 1$ and $T_u = 358$ K. The flame temperature of benzene is also reported as a reference. A monotonic decrease in the flame

temperature is observed when H/C ratio of the fuel increases. Benzene (no saturated C atom) has the lowest H/C ratio of the fuels here considered and the hottest flame. Toluene, presents the second hottest flame, followed by the other alkyl aromatics. Also shown in Figure 5 are the computed flame speeds at the same conditions (panel a, solid bars). Although toluene has the second highest flame temperature of the fuel series, it has the lowest flame speed. This mismatch between the flame temperatures and the measured/calculated burning velocities calls for a deeper explanation for the trends observed in Figure 5. In order to separate the thermodynamic aspects from the kinetics of these fuels, a new set of calculations was performed numerically by altering the heat capacity of the inert so that all the flames had the same post-flame temperature. A similar procedure has been applied in previous experimental studies by tailoring the inert composition using argon and nitrogen to alter heat capacity of the inert. However, this approach also changes the reaction rate constants of reactions that have third bodies where each third body has a different collision efficiency. Although this issue cannot be avoided experimentally, Milano's group recently avoided this problem computationally by altering the heat capacity of nitrogen to set the adiabatic flame temperature to 2300 K ($T_u = 298$ K) for a series of hydrocarbon flames [25]. This approach allows modelers to directly compare the kinetics of different fuels while maintaining the same post-flame temperature and inert composition, and without affecting some reaction rate constants through third body interactions.

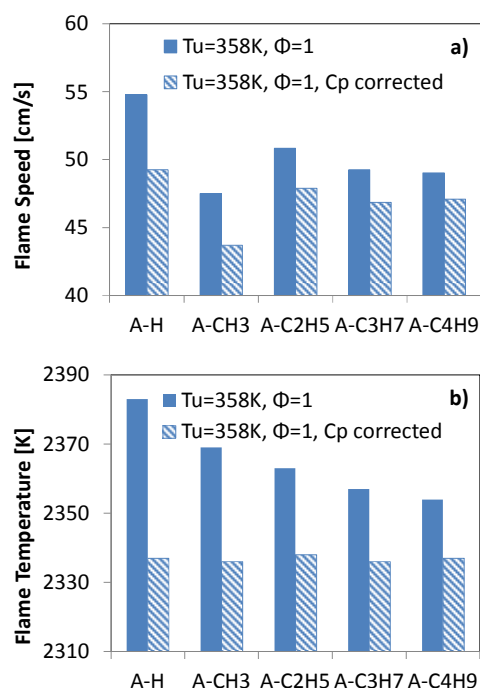


Figure 5: Comparison of adiabatic burning velocities (panel a) and temperatures (panel b) across five aromatic species: solid bars: original mechanism; striped bars: modified mechanism using corrected C_p for nitrogen to have an adiabatic flame temperature of 2300 K with $T_u = 298$ K. The symbol A- represents the phenyl group (C_6H_5-).

To achieve this direct comparison, the original thermodynamic properties of nitrogen were recomputed for each fuel after multiplying the $C_p(T)$ function by corrective coefficient to compensate for the heat of combustion. Figure 5a shows the flame speeds of the five fuels using the original thermodynamic files (solid bars) and the artificial heat capacities at stoichiometric conditions and $T_u = 358$ K (striped bars). The trend observed in the original calculation is mostly conserved even though the differences between benzene, ethyl-benzene, *n*-propyl-benzene and *n*-butyl-benzene are now somewhat reduced. On the other hand, now that the high flame temperature does not partially compensate for its lower flame speed, toluene consolidates its role as an outlier, being significantly less reactive than benzene and ethyl-benzene. These observations are in good agreement with what highlighted both by Ji et al. and Hui et al. [4,5] who compared toluene and *n*-propyl-benzene in a

counter-flow flame configuration. This new set of experiments and calculations extends their results and place toluene behavior in the broader context of the *n*-alkyl aromatics. The temperature compensated results show that the differences in flame speeds for this series of aromatics is mainly due to differences in chemical kinetics and not due to differences in post-flame temperatures. In the next section, the effect of the differences chemical kinetics on the flame speeds is investigated.

Using Chemkin Pro[®], an A-factor sensitivity analysis on the inlet velocity was performed at the same conditions reported in Figure 5. The modified thermodynamic properties were used in order to isolate the reactions relevant to the observed behavior. The results of the analysis were filtered by relative importance of the reactions and percentile variation across the different alkyl-aromatics (benzene was included in the analysis but is not reported). For example, reactions involving phenyl radical showed high sensitivity coefficients, but are not shown in Figure 5 because the magnitude of the sensitivity coefficient is similar for each of the alkyl benzene in the series. After ranking all the reactions by their absolute A-sensitivity factor values and filtering out the reaction steps showing only minor differences across the different fuels (less than 40%), the histogram in Figure 6 was obtained.

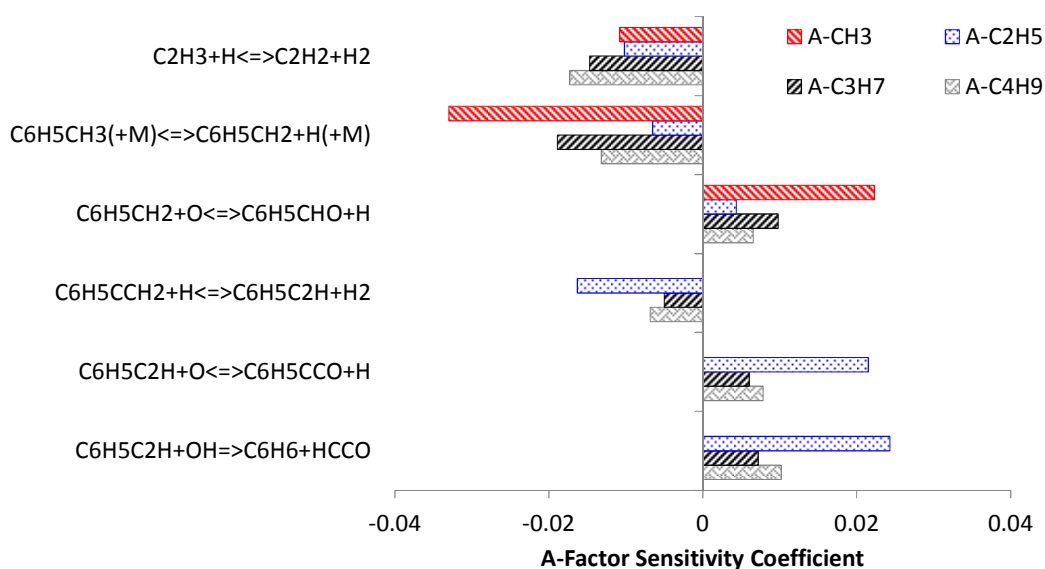


Figure 6: A-sensitivity factor analysis on the flame speed of four alkyl-benzenes: toluene, ethylbenzene, *n*-propylbenzene, *n*-butylbenzene using modified heat capacities for nitrogen. $T_u = 358$, $\Phi = 1$, flame temperature is $2337 \text{ K} \pm 1 \text{ K}$ for all the case. The symbol A-represents the phenyl group (C_6H_5-).

It should be noted that the most sensitive reaction shown in Figure 6 (the benzyl + H initiation/termination step) has a sensitivity coefficient in the order of 0.033 whereas the highest sensitive reaction for all the fuels is the classical $\text{H} + \text{O}_2 \rightleftharpoons \text{OH} + \text{H}$ reaction, which has a sensitivity coefficient in the order of 0.36 (more than 10 times higher!) with very little variation across all the fuels.

Although the overall flame speed is controlled by the chemistry of small radicals, as in other systems, the burning velocities of aromatics were found to be influenced by fuel specific intermediates such as phenyl, benzyl, or even heavier species. While the relative importance of the phenyl radical appears to be similar for all the alkyl aromatic species (and therefore was filtered out during the processing of the sensitivity results), two aromatic species can be identified as important in controlling the differences among the reactivity of the fuels: the benzyl radical and phenyl-acetylene, an intermediate particularly abundant in ethylbenzene oxidation. Phenyl-acetylene is formed from the production of secondary benzyl radicals in alkylbenzene flames when the side chain is longer than one carbon group. Secondary benzyl radicals react either by β -scission or reaction with O_2 . In the case of a C_2 side chain, both

pathways result in styrene formation which dehydrogenates to phenyl-acetylene. The reactions of phenyl-acetylene with H, O and OH appearing in the analysis shown in Figure 6, are controlling steps in the oxidation of the side chain of ethyl-benzene, and significantly influence its flame speed.

More interesting for the purpose of our investigation is the role of the benzyl radical ($C_6H_5CH_2$). Contrarily to what happened with secondary benzylic radicals, which can undergo fast unimolecular and oxidative consumption pathways, the $C_6H_5CH_2$ radical concentration tends to buildup, due to its intrinsic stability, in the region ahead of the flame front. The high concentration of resonantly stabilized radicals interferes with the back-diffusing H radicals, scavenging them, and effectively changing the ratio between reactive and unreactive radicals that compose the radical pool. Figure 7 compares the concentration of $C_6H_5CH_2$ radical in proximity of the flame front across the five fuels here considered. The relative concentration of benzyl radicals correlates inversely with the trend in the flame speeds observed in the calculations and the experiments: low $C_6H_5CH_2$ concentrations peaks correspond to high flame speeds. Similar evidences of the impact of benzyl radicals on burning propensities were indicated by [4,5,26].

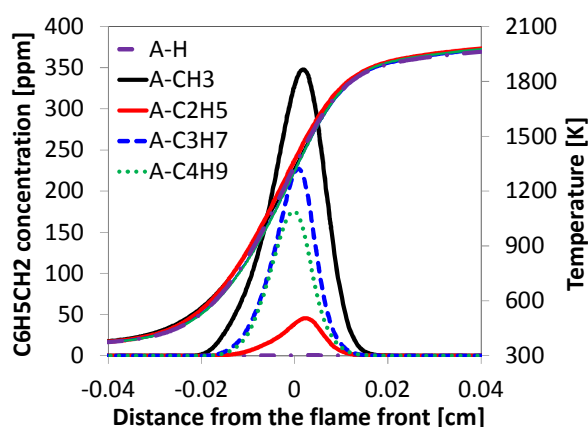


Figure 7: Concentration profiles of the $C_6H_5CH_2$ radical in proximity of the flame front for the five fuels considered in our analysis. The symbol A-represents the phenyl group (C_6H_5-). (For the benzene flame, the concentration of benzyl radical is negligible).

The different propensity of the five fuels to form benzyl radical can be explained on the basis of their kinetics. Not surprisingly benzene has very little propensity to form benzyl radicals because of the complex mechanism required to add a carbon to the ring, process which is not favored in a hot oxidizing environment such as the one obtained in a premix flame.

Toluene can produce large amounts of benzyl radicals via abstraction and initiation reactions, with the first one being largely dominant in an oxidizing environment. Abstraction reactions on the benzylic site are favored compared to other fuel consuming reactions by the weak C-H benzylic bonds and represent the main consumption pathway for toluene through all the combustion process at stoichiometric conditions. As a result reactive radicals ($H\bullet$, $\bullet O\bullet$ or $\bullet OH$) are neutralized by the abstraction on the R- CH_3 group and the benzyl radical scavenges H radicals via radical recombination at low temperature. In the case of heavier alkyl aromatics, benzyl radicals are generated via initiation reactions or by an abstraction/decomposition sequence. The initiation is the only pathway available to ethyl-benzene to generate $C_6H_5CH_2$ radicals. *n*-Propyl-benzene and *n*-butyl-benzene, on the other hand, can undergo abstraction reactions on the primary and secondary carbons of the alkyl chains followed by β -scission reactions leading to benzyl radicals and an alkene. The overall activation energy required by the multistep process is significantly lower than the energy needed to break a C-C bond (according to the LLNL detailed kinetic mechanism the β -scission decomposition reactions leading to $C_6H_5CH_2$ formation require activation energies in the order of 25,000 cal/mol, initiation reactions

involving the C-C bond require about 75,000 cal/mol) and therefore allows for benzyl radicals formation at relatively low temperatures, resulting in a broader and higher peaks of these non-reactive radicals near the flame front. The lower activation energy required by the two-step process compared with the initiation step also explains why the location of the $C_6H_5CH_2$ radical peaks is different for toluene, *n*-propyl-benzene and *n*-butyl-benzene when compared to ethyl-benzene.

5. Conclusions

New experimental data covering the burning velocities of several components belonging to the aromatic class of hydrocarbons found in diesel fuels were measured using the heat flux method (e.g. ethyl-, *n*-propyl- and *n*-butyl-benzenes). These data are extremely relevant to the development of systematic models describing chemistry of large alkyl-aromatics, especially if the paucity of the existing literature on the subject is considered. The data obtained in this study were compared with the few existing literature data. Unfortunately the only data available for comparison were laminar flame speeds of *n*-propyl-benzene. Some discrepancies between the newly measured data and the existing literature data were highlighted suggesting that new measurements obtained with different types of methods are necessary to confirm the values of laminar flame velocities of *n*-propyl-benzene and other fuels belonging to its family.

Comparisons of experimental data obtained in this study showed that the laminar flame velocities of alkyl-benzenes larger than ethyl-benzene are relatively similar but, when smaller differences across the fuels are considered, some interesting trends emerge. Experimental data were also compared with data computed using a detailed chemical kinetic model. Predictions obtained with the LLNL kinetic model for alkyl-benzenes were in very good agreement with experimental data measured in this study. The predictions obtained with the model, which was built upon a systematic set of reaction rules consistent across all the fuels, reinforced the confidence in the validity of the observed trends which were identically reproduced in the calculations.

The kinetic mechanism was used to analyze the chemistry controlling the flame speed. Thermodynamic effects rising from the different heat of combustion of the fuels were isolated and off-set by altering the heat capacity of the inert. Artificial thermodynamic properties were obtained for nitrogen so that the flame temperature of all the fuels was the same. The trend observed in the computed flame speeds remained after these changes, suggesting that kinetics was responsible for the differences in flame speed. Sensitivity analysis and reaction path analysis were performed and species concentrations were computed. These numerical results showed that the chemistry of the resonantly stabilized radicals (in particular the benzyl radicals) is responsible for the differences in burning velocities observed among toluene, ethyl-benzene, *n*-propyl-benzene and *n*-butyl-benzene. A higher propensity to form benzyl radicals results in a lower burning velocity. The model allowed isolation of the reaction pathways controlling the benzyl radical formation. While heavier alkyl-benzenes produce benzyl radicals primarily via initiation and β -scission decomposition reactions of their alkyl radicals (this last options though requires a side chain of at least three carbon atoms), toluene can directly generate $C_6H_5CH_2\bullet$ through the abstraction of the weakly-bonded benzylic hydrogen atoms. The resulting high concentration of benzyl radicals in the pre-flame zone inhibits the flame propagation and reduces the burning velocity: small radicals that back diffuse from the flame region are consumed via abstraction reactions and benzyl radicals scavenge H atoms via termination reaction.

Acknowledgements

The work performed at Université de Lorraine-CNRS was supported by Saudi Aramco. The modeling work performed at LLNL was supported by U.S. Department of Energy, Office of Vehicle Technologies, and performed under the auspices of the U.S. Department of Energy by Lawrence Livermore National

Laboratory under Contract DE-AC52-07NA27344. The authors thank the program manager Gurpreet Singh for his support.

Supplemental data

The detailed kinetic model used for running simulations is given as supplemental data (mechanism, thermodynamic properties and transport properties).

References

- [1] J.T. Farrell, N.P. Cernansky, F.L. Dryer, C.K. Law, D.G. Friend, C.A. Hergart, R.M. McDavid, A.K. Patel, C.J. Mueller, H. Pitsch, Development of an Experimental Database and Kinetic Models for Surrogate Diesel Fuels, SAE International, Warrendale, PA (2007)
- [2] W.J. Pitz, C.J. Mueller, *Prog. Energ. Combust. Sci.*, 37 (2011), pp. 330–350
- [3] C.J. Mueller, W.J. Cannella, T.J. Bruno, B. Bunting, H.D. Dettman, J.A. Franz, M.L. Huber, M. Natarajan, W.J. Pitz, M.A. Ratcliff, K. Wright, *Energ. Fuels*, 26 (6) (2012), pp. 3284–3303
- [4] X. Hui, A.K. Das, K. Kumar, C.-J. Sung, S. Dooley, F.L. Dryer, *Fuel*, 97 (2012), pp. 695–702
- [5] C. Ji, E. Dames, H. Wang, F.N. Egolfopoulos, *Combust. Flame*, 159 (2012), pp. 1070–1081
- [6] X. Hui, C.-J. Sung, *Fuel*, 109 (2013), pp. 191–200
- [7] T. Malewicki, S. Gudiyella, K. Brezinsky, *Combust. Flame*, 160 (2013), pp. 17–30
- [8] S. Dooley, S.H. Won, J. Heyne, T.I. Farouk, Y. Ju, F.L. Dryer, K. Kumar, X. Hui, C.-J. Sung, H. Wang, M. A. Oehlschlaeger, V. Iyer, S. Iyer, T.A. Litzinger, R.J. Santoro, T. Malewicki, K. Brezinsky, *Combust. Flame*, 159 (2012), pp. 1444–1466
- [9] A. Mze-Ahmed, P. Dagaut, K. Hadj-Ali, G. Dayma, *Energ. Fuels*, 26 (2012), pp. 6070–6079
- [10] E. Pousse, P.A. Glaude, R. Fournet, F. Battin-Leclerc, *Combust. Flame*, 156 (2009), pp. 954–974
- [11] P. Dievart, P. Dagaut, *Proc. Combust. Inst.*, 33 (2011), pp. 209–216
- [12] B. Husson, R. Bounaceur, K. Tanaka, M. Ferrari, O. Herbinet, P.A. Glaude, R. Fournet, F. Battin-Leclerc, M. Crochet, G. Vanhove, R. Minetti, C.J. Tobin, K. Yasunaga, J.M. Simmie, H.J. Curran, T. Niass, O. Mathieu, S.S. Ahmed, *Combust. Flame*, 159 (2012), pp. 1399–1416
- [13] L.H.P. De Goey, A. Van Maaren, R.M. Quax, *Combust. Sci. Technol.*, 92 (1993), pp. 201–207
- [14] A. Van Maaren, D.S. Thung, L.H.P. De Goey, *Combust. Sci. Technol.*, 96 (1994), pp. 327–344
- [15] I.V. Dyakov, A.A. Konnov, J. De Ruyck, K.J. Bosschaart, E.C.M. Brock, L.P.H. De Goey, *Combust. Sci. Technol.*, 172 (2001), pp. 81–96
- [16] A.A. Konnov, I.V. Dyakov, J. De Ruyck, *Exp. Therm. Fluid Sci.*, 27 (2003), pp. 379–384
- [17] K.J. Bosschaart, L.P.H. De Goey, *Combust. Sci. Technol.*, 176 (2004), pp. 1537–1564
- [18] P. Dirrenberger, H. Le Gall, R. Bounaceur, O. Herbinet, P.-A. Glaude, A. Konnov, F. Battin-Leclerc, *Energ. Fuels*, 25 (2011), pp. 3875–3884
- [19] P. Dirrenberger; P.-A. Glaude; R. Bounaceur; H. Le Gall; A. Pires da Cruz; A. Konnov; F. Battin-Leclerc, *Fuel*, 115 (2014), pp. 162–169
- [20] D. Darcy, C.J. Tobin, K. Yasunaga, J. M. Simmie, J. Wurmel, W.K. Metcalfe, T. Niass, S.S. Ahmed, C.K. Westbrook, H.J. Curran, *Combust. Flame*, 159 (2012), pp. 2219–2232
- [21] D. Darcy, M. Mehl, J.M. Simmie, J. Wurmel, W.K. Metcalfe, C.K. Westbrook, W.J. Pitz, H.J. Curran, *Proc. Combust. Inst.*, 34 (2013), pp. 411–418
- [22] H. Nakamura, D. Darcy, M. Mehl, C.J. Tobin, W.K. Metcalfe, W.J. Pitz, C.K. Westbrook, H.J. Curran, *Combust. Flame*, 161 (2014), pp. 49–64
- [23] D. Darcy, H. Nakamura, C.J. Tobin, M. Mehl, W.K. Metcalfe, W.J. Pitz, C.K. Westbrook, H.J. Curran, *Combust. Flame*, 161 (2014), pp. 65–74
- [24] W.K. Metcalfe, S. Dooley, F.L. Dryer, *Energ. Fuels*, 25 (2011), pp. 4915–4936
- [25] E. Ranzi, A. Frassoldati, R. Grana, A. Cuoci, T. Faravelli, A.P. Kelley, C.K. Law, *Prog. Energ. Combust. Sci.*, 38 (2012), pp. 468–501
- [26] S.H. Won, W. Sun, Y. Ju, *Combust. Flame*, 157 (2010), pp. 411–420